

## Particle Swarm Optimization Based Damage Detection Method For Beam Type Structures Subject To Moving Vehicle

\*Hakan Gökdağ<sup>1)</sup>

<sup>1)</sup> Department of Mechanical Engineering, Bursa Technical University,  
Bursa 16190, Turkey

<sup>1)</sup> [hakan.gokdag@btu.edu.tr](mailto:hakan.gokdag@btu.edu.tr)

### ABSTRACT

In this work a crack identification method for bridge type structures under moving vehicle is proposed. The basic of the method is to formulate damage detection as an inverse problem, and solve for damage locations and extents. To this end, an objective function is defined based on the difference of damaged beam dynamic response and the response calculated by the mathematical model of the beam. The optimization problem is solved through a popular evolutionary algorithm, i.e. the particle swarm optimization (PSO) with linearly increasing inertia weight, to obtain crack locations and depths. From the numerical simulations it was observed that cracks with depth ratio of 0.1 can be identified with the present method in spite of three percent noise interference and distortive effect of road surface roughness.

**Key Words:** Cracked beam, damage detection, particle swarm optimization, moving vehicle

### 1. INTRODUCTION

Structures subject to vehicular loads have many practical applications such as railway tracks, bridges, roadways, etc. Since moving load yields larger deflections and higher stresses than equivalent static load conditions, dynamics of such structures has received considerable attention in the literature (Frýba 1999). If the carrying structure has crack-like local defects, then the impact of moving load becomes more pronounced. In the earlier study on this issue Mahmoud (2001) demonstrated that crack shifts the minimum point of displacement to the right-hand on the time axis. Bilello and Bergman (2004) concluded that changes in the time-response of the beam due to damage are more perceptible in comparison to the changes in the natural frequencies. Law and Zhu (2004) investigated the effects of open and breathing cracks on the response of concrete bridges carrying moving vehicle. Ariaei et al. (2009) performed a similar study for beams with breathing cracks subject to moving mass. On the other hand, various damage detection methods have been developed for beams

---

<sup>1)</sup> Assis. Professor

subject to moving load/vehicle using the continuous wavelet transform (CWT) (Zhu and Law 2006; Nguyen and Tran 2010; Hester and Gonzalez 2011; Gökdağ 2011; Khorram et al. 2012). They are based on the fact that CWT coefficients of beam dynamic response demonstrate local peaks at crack locations, and magnitudes of these peaks are proportional to crack depths.

In structural damage detection there are other methods based on model updating. The basic of these is to update mathematical or finite element model of the structure to match the calculated response to the one measured from damaged structure. This is achieved through an optimization procedure. To solve the optimization problem evolutionary methods are generally preferred, as they do not require gradient calculation, and have less possibility of being trapped by local minima in comparison with the gradient based methods (Begambre and Laier 2009; Buezas et al 2010; Moradi et al 2011; Seyedpoor 2012). One of these algorithms is the particle swarm optimization (PSO). PSO, developed by Kennedy and Eberhart (1995), is a stochastic optimization technique inspired by natural flocking and swarm behavior of birds and insects. It is known to have less parameters and rapid convergence compared with the genetic algorithms (GA) (Parsopoulos and Vrahatis 2010), and has been successfully employed in model updating based damage detection applications (Begambre and Laier 2009; Moradi et al 2011; Seyedpoor 2012). In model updating based damage detection, time dependent structural response is used, as well. Buezas et al. (2010) formulated an optimization problem using time responses from several points on the beam, and determined crack size and depth by solving this problem.

In the present work, motivated by the conclusion of Bilello and Bergman (2004) mentioned above and the method of Buezas et al. (2010), a model update based damage detection approach has been proposed for bridge type structures carrying moving vehicle. In this respect, time dependent deflections from several points on a cracked beam were obtained, and an objective function was defined by subtracting these from the ones calculated by the mathematical model of the structure. Then, the PSO is employed to minimize this objective function to determine crack locations and depths. To the best of the author's knowledge, this is the first study dealing with the formulation of damage detection in a beam subject to moving vehicle as an inverse problem and solving by the PSO with increasing inertia weight for crack identification.

## 2. MATERIAL AND METHOD

### 2.1. Dynamic response of the beam

Fig.1 illustrates the beam-vehicle system. The Euler-Bernoulli model is considered for the beam, and half car model is adopted for the vehicle moving with the speed  $V$ . An open crack with depth  $h_1$  is located at  $z_1$  on the beam. Surface unevenness of the beam is regarded and tyres are assumed to be always in contact with the beam. Under these assumptions the equations of motion for the vehicle and beam can be derived as follows:

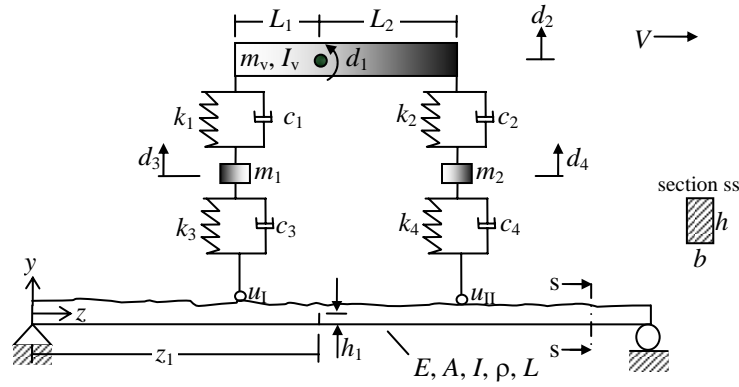


Fig. 1. Beam-vehicle system.

$$\begin{bmatrix} I_v & 0 & 0 & 0 \\ 0 & m_v & 0 & 0 \\ 0 & 0 & m_1 & 0 \\ 0 & 0 & 0 & m_2 \end{bmatrix} \begin{Bmatrix} \ddot{d}_1 \\ \ddot{d}_2 \\ \ddot{d}_3 \\ \ddot{d}_4 \end{Bmatrix} + \begin{bmatrix} c_1 L_1^2 + c_2 L_2^2 & L_2 c_2 - L_1 c_1 & L_1 c_1 & -L_2 c_2 \\ L_2 c_2 - L_1 c_1 & c_2 + c_1 & -c_1 & -c_2 \\ L_1 c_1 & -c_1 & c_3 + c_1 & 0 \\ -L_2 c_2 & -c_2 & 0 & c_2 + c_4 \end{bmatrix} \begin{Bmatrix} \dot{d}_1 \\ \dot{d}_2 \\ \dot{d}_3 \\ \dot{d}_4 \end{Bmatrix} + \begin{bmatrix} k_1 L_1^2 + k_2 L_2^2 & L_2 k_2 - L_1 k_1 & L_1 k_1 & -L_2 k_2 \\ L_2 k_2 - L_1 k_1 & k_2 + k_1 & -k_1 & -k_2 \\ L_1 k_1 & -k_1 & k_3 + k_1 & 0 \\ -L_2 k_2 & -k_2 & 0 & k_2 + k_4 \end{bmatrix} \begin{Bmatrix} d_1 \\ d_2 \\ d_3 \\ d_4 \end{Bmatrix} = \begin{Bmatrix} 0 \\ 0 \\ k_3 \delta_I(u+r) + c_3 \delta_I(\dot{u} + r'V) \\ k_4 \delta_{II}(u+r) + c_4 \delta_{II}(\dot{u} + r'V) \end{Bmatrix} \quad (1)$$

$$\rho A \frac{\partial^2 y(z,t)}{\partial t^2} + C \frac{\partial y(z,t)}{\partial t} + EI \frac{\partial^4 y(z,t)}{\partial x^4} = -P_I \delta_I - P_{II} \delta_{II} \quad (2)$$

where  $I_v, m_v, m_1, m_2, L_1, L_2, k_1, k_2, k_3, c_1, c_2, c_3, c_4$  are vehicle parameters shown in Fig.1,  $C$  is the damping of beam material.  $d_i, i=1:4$ , denote vehicle degrees of freedom,  $\delta_I$  and  $\delta_{II}$  are the Dirac delta functions defined as  $\delta_{II} = \delta(z-Vt)$ ,  $\delta_I = \delta(z-Vt-(L_1+L_2))$ .  $P_I$  and  $P_{II}$  are the interaction forces acting on the beam through the contact points I and II, as follows:

$$P_I = \left( m_1 + \frac{L_2}{L_1+L_2} m_v \right) 9.81 + k_3(u+r-d_3) + c_3(\dot{u} + r'V - \dot{d}_3) \quad (3a)$$

$$P_{II} = \left( m_2 + \frac{L_1}{L_1+L_2} m_v \right) 9.81 + k_4(u+r-d_4) + c_4(\dot{u} + r'V - \dot{d}_4) \quad (3b)$$

where  $u$  is the vertical displacement at the tyre contact point, i.e.  $u = y(z, t)$ , its derivative with respect to time is  $\dot{u} = d(y(z, t))/dt = V\partial y(z, t)/\partial z + \partial y(z, t)/\partial t$ , and  $' = d/dz$ . Road surface roughness function in Eq. (3) is (Wu and Law 2011)

$$r(z) = \sum_{k=1}^N \left[ \left( 4S_d(f_0) \left( \frac{2\pi k}{L_c f_0} \right)^{-2} \frac{2\pi}{L_c} \right)^{1/2} \cos \left( \frac{2\pi k f_0}{L_c} z + \theta_k \right) \right] \quad (4)$$

where  $S_d(f_0)$  is the roughness coefficient in  $m^3/\text{cycles}$ ,  $f_0$  is the discontinuity frequency equal to  $1/2\pi$  (cycle/m),  $L_c$  is twice the length of the beam, and  $\theta_k$  is the uniform random number between 0 and  $2\pi$ .  $N=10^4$  is adopted in this study. The road classification according to the ISO standard is based on the value of roughness coefficient. Five classes representing different qualities of the road are A: very good, B: good, C: average, D: poor, E: very poor with the roughness coefficients equal to  $1 \times 10^{-6}$ ,  $6 \times 10^{-6}$ ,  $16 \times 10^{-6}$ ,  $64 \times 10^{-6}$ ,  $256 \times 10^{-6}$ , respectively.

Assuming mode superposition, i.e.  $\mathbf{Y}(z)^T \mathbf{q}(t)$ , substituting into Eq.(2), multiplying by  $\mathbf{Y}(z)$  and integrating from 0 to  $L$ , and finally combining with Eq.(1) lead to the following coupled beam-vehicle equations:

$$\begin{bmatrix} \mathbf{M}_{N_m \times N_m} & \mathbf{0}_{N_m \times 4} \\ \mathbf{0}_{4 \times N_m} & \bar{\mathbf{M}}_{4 \times 4} \end{bmatrix} \begin{Bmatrix} \ddot{\mathbf{q}} \\ \ddot{\mathbf{d}} \end{Bmatrix} + \begin{bmatrix} \mathbf{C} + \bar{\mathbf{A}}_8 & \bar{\mathbf{A}}_{10} \\ -\mathbf{A}_6 & \bar{\mathbf{C}} \end{bmatrix} \begin{Bmatrix} \dot{\mathbf{q}} \\ \dot{\mathbf{d}} \end{Bmatrix} + \begin{bmatrix} \mathbf{K} + \bar{\mathbf{A}}_7 & \bar{\mathbf{A}}_9 \\ -\mathbf{A}_5 & \bar{\mathbf{K}} \end{bmatrix} \begin{Bmatrix} \mathbf{q} \\ \mathbf{d} \end{Bmatrix} = \begin{Bmatrix} \mathbf{F}_1 \\ \mathbf{F}_2 \end{Bmatrix} \quad (5)$$

where  $\mathbf{M} = \int_0^L \rho A \mathbf{Y} \mathbf{Y}^T dz$ ,  $\mathbf{C} = \int_0^L C \mathbf{Y} \mathbf{Y}^T dz$ ,  $\mathbf{K} = \int_0^L EI \mathbf{Y} \mathbf{Y}^T dz$ .  $\bar{\mathbf{M}}, \bar{\mathbf{C}}, \bar{\mathbf{K}}$  are the mass, damping and stiffness matrices in Eq.(1),  $N_m$  is the number of modes used,  $\mathbf{Y}(z)$  is the vector of size  $N_m \times 1$  containing vibration modes of the cracked beam, and  $\mathbf{q}(t)$  stands for the modal coordinates. Additionally,

$$\mathbf{A}_1 = [\mathbf{Y}(z)^T k_3 + V c_3 \mathbf{Y}'(z)^T] \delta_I, \quad \mathbf{A}_2 = [\mathbf{Y}(z)^T c_3] \delta_I \quad (6a)$$

$$\mathbf{A}_3 = [\mathbf{Y}(z)^T k_4 + V c_4 \mathbf{Y}'(z)^T] \delta_{II}, \quad \mathbf{A}_4 = [\mathbf{Y}(z)^T c_4] \delta_{II} \quad (6b)$$

$$\mathbf{A}_5 = \begin{bmatrix} \mathbf{0}_{2 \times N_m} \\ \mathbf{A}_1 \\ \mathbf{A}_2 \end{bmatrix}, \quad \mathbf{A}_6 = \begin{bmatrix} \mathbf{0}_{2 \times N_m} \\ \mathbf{A}_2 \\ \mathbf{A}_4 \end{bmatrix}, \quad \bar{\mathbf{A}}_j = \int_0^L \mathbf{Y}(z) \mathbf{A}_j dz, \quad j=7,8,9,10 \quad (6c)$$

$$\mathbf{A}_7 = \mathbf{A}_1 + \mathbf{A}_3, \quad \mathbf{A}_8 = \mathbf{A}_2 + \mathbf{A}_4, \quad \mathbf{A}_9 = [0 \quad 0 \quad -k_3 \quad -k_4], \quad \mathbf{A}_{10} = [0 \quad 0 \quad -c_3 \quad -c_4] \quad (6d)$$

$$\mathbf{F}_1 = \int_0^L \mathbf{Y}(z) \left( [W_1 + rk_3 + r'Vc_3] \delta_I + [W_2 + rk_4 + r'Vc_4] \delta_{II} \right) dz, \quad (6e)$$

$$W_I = \left( m_1 + \frac{L_2}{L_1 + L_2} m_v \right) 9.81, \quad W_{II} = \left( m_2 + \frac{L_1}{L_1 + L_2} m_v \right) 9.81, \quad (6f)$$

$$\mathbf{F}_2 = [0 \quad 0 \quad (rk_3 + r'Vc_3) \delta_I \quad (rk_4 + r'Vc_4) \delta_{II}]^T \quad (6g)$$

Eq.(5) can be solved by any numerical integration method. In this study Newmark- $\beta$  method (with  $\beta=1/6$  and  $\gamma=1/2$  (Clough and Penzien 1995)) is employed for this purpose. Before solving the equation, vibration modes of the cracked beam is required to obtain the coefficient matrices in Eq. (5). Assuming the beam is composed of two parts joined at the crack location through a rotational spring, we can write the following compatibility equations at the crack location (Mahmoud 2001):

$$Y_1(z_1) = Y_2(z_1), \quad Y_1'(z_1) + \theta Y_1''(z_1) = Y_2'(z_1), \quad Y_1''(z_1) = Y_2''(z_1), \quad Y_1'''(z_1) = Y_2'''(z_1) \quad (7)$$

Here  $Y_i(z)$  is the mode shape of the  $i$ th beam part defined as follows

$$Y_i(z) = C_{i1} \cos(\lambda z) + C_{i2} \sin(\lambda z) + C_{i3} \cosh(\lambda z) + C_{i4} \sinh(\lambda z), \quad i=1,2 \quad (8)$$

where  $\lambda = (\rho A \omega^2 / EI)^{0.25}$ .  $\lambda$  and  $\omega$  are eigenvalue and natural frequency parameters, respectively, and  $C_{ij}$  are the constants to be determined by solving the eigenvalue problem. The geometric factor of the crack,  $\theta$ , is defined as follows (Mahmoud 2001; Ariaei et al 2009)

$$\theta = 2h \left( \frac{\bar{h}_1}{1 - \bar{h}_1} \right)^2 \left( 5.93 - 19.69\bar{h}_1 + 37.14\bar{h}_1^2 - 35.84\bar{h}_1^3 + 13.12\bar{h}_1^4 \right), \quad \bar{h}_1 = h_1/h \quad (9)$$

The eigenvalue problem is formulated using Eq.(7) along with the boundary conditions for the simple supports. Note that in the case of multiple cracks the number of Eq. (8) is equal to the number of cracks. Natural frequencies and vibration modes of the cracked beam can be obtained by solving the eigenvalue problem (see Mahmoud 2001, Ariaei et al 2009, Zhu and Law 2006, Gökdağ 2011 for details). Using these vibration modes Eq.(5) is solved. Fig.2 illustrates the normalized midspan deflection of the beam. The following numerical data for the beam-vehicle system are employed to obtain the figure (Nguyen and Tran 2010):  $E = 210$  GPa,  $\rho = 7855$  kgm<sup>-3</sup>,  $L=50$ m,  $b=1$ m,  $h=2$ m,  $m_v = 12404$  kg,  $m_1 = m_2 = 725.4$  kg,  $I_v = 172160$  kgm<sup>2</sup>,  $k_1 = 1969034$  Nm<sup>-1</sup>,  $k_2 = 727812$  Nm<sup>-1</sup>,  $k_3 = 4735000$  Nm<sup>-1</sup>,  $k_4 = 1972900$  Nm<sup>-1</sup>,  $c_1 = 7181.8$  Nsm<sup>-1</sup>,  $c_2 = 2189.6$  Nsm<sup>-1</sup>,

$c_3 = c_4 = 0$ ,  $L_1 = L_2 = 3\text{m}$ . Normalization is made by dividing to the midspan deflection of the simply-supported beam loaded by concentrated static force  $P$  acting on the midspan, i.e.  $PL^3/(48EI)$  where  $P=9.81(m_v + m_1 + m_2)$ . The first six vibration modes of the beam, for which the natural frequencies are 1.88, 7.50, 16.88, 30.01, 46.89, 67.52 Hz, are employed. Two percent modal damping is considered for each mode (Zhu and Law 2006). The moving load speed is  $V=10\text{m/s}$ . The sampling frequency of the simulation is 500 Hz which can capture the response of the first six vibration modes of the beam. The roughness coefficient is  $S_d(f_0)=16\times 10^{-6}$  and damage locations are  $\bar{z}_1 = z_1/L=0.33$ ,  $\bar{z}_2 = z_2/L=0.67$  with equal crack depth  $\bar{h}_1 = h_1/h=0.2$ ,  $\bar{h}_2 = h_2/h=0.2$ . From Fig.2 it is seen that damage and roughness have significant impact on the maximum amplitude and variation of deflection with time.

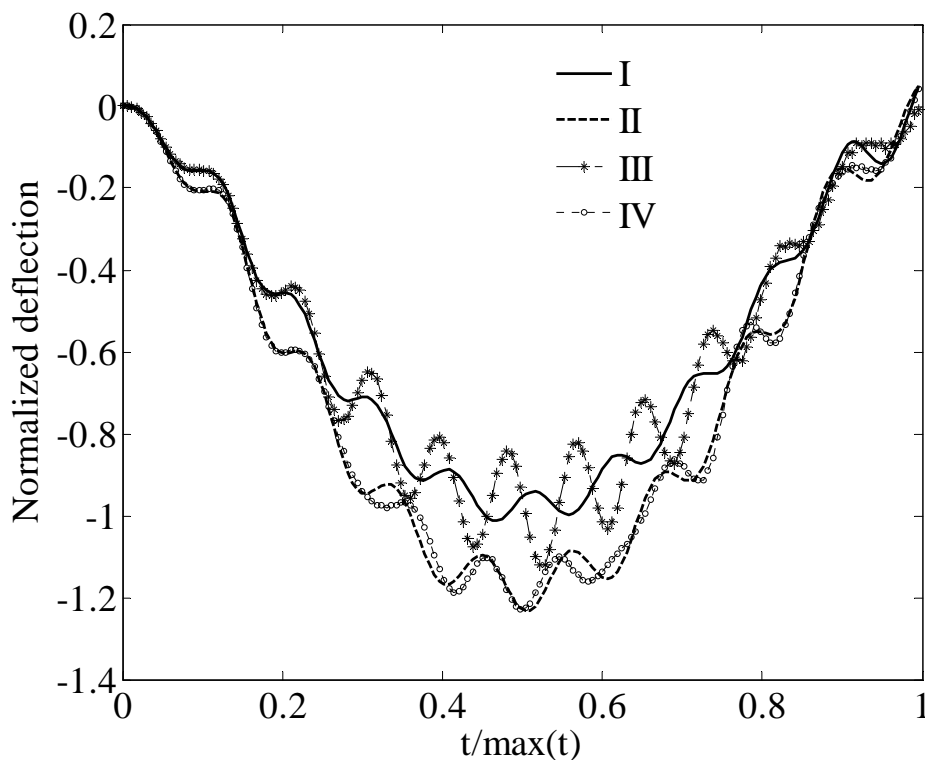


Fig. 2. Normalized midspan deflections of the beam. I: damage (-), roughness (-), II: damage (+), roughness (-). III: damage (-), roughness (+), IV: damage (+), roughness (+). (-): not present, (+): present

## 2.2. The objective function and the constrains

The aim is to correlate the response of the damaged beam to the one calculated by the mathematical model of the structure, so that crack locations and depths can be determined. To achieve this, it is proposed to adjust crack sizes and locations by

solving an optimization problem. The objective function of the problem is introduced as follows:

$$f(\mathbf{x}) = \sum_{n=1}^{N_{mp}} \int_0^T \frac{|y(z_n, t) - \bar{y}(z_n, t)|}{\max(|\bar{y}(z_n, t)|)} dt \quad (10)$$

where  $N_{mp}$  is the number of measurement points on the beam,  $z_n$  is the location of the  $n$ th measurement point on the beam,  $\bar{y}$  denotes the reference displacements measured from damaged beam,  $y$  stands for the corresponding displacements computed by the mathematical model of the structure.  $T$  is the total time for the vehicle to move across the beam.  $\mathbf{x}$  is the vector containing crack location and size parameters, i.e.

$$\mathbf{x} = \left\{ \bar{h}_1, \bar{h}_2, \dots, \bar{h}_{N_c}, \bar{z}_1, \bar{z}_2, \dots, \bar{z}_{N_c} \right\}, \quad \bar{h}_i = \frac{h_i}{h}, \quad \bar{z}_i = \frac{z_i}{L} \quad (11)$$

where  $N_c$  denotes the number of cracks. As to the measurement points, it is better to chose them close to the midpoint, since maximum deflection occurs at the beam midspan. Thus, four points (Buezas et al 2010) on the beam were determined as  $\{0.3 \ 0.5 \ 0.6 \ 0.7\}L$ , i.e.  $N_{mp} = 4$  in Eq. (10). If the number of cracks ( $N_c$ ) is more than one, then extra constraints other than lower and upper boundaries should be introduced for the optimization algorithm to make search in the feasible region. With these explanations in mind, the optimization problem can be formulated as follows

$$\left. \begin{array}{l} \min f(\mathbf{x}) \\ \text{subject to:} \\ \bar{z}_i - \bar{z}_{i+1} < 0, \quad i = 1, 2, \dots, N_c - 1 \\ 0 < \bar{z}_j < 1, \quad 0 \leq \bar{h}_j < 1, \quad j = 1, 2, \dots, N_c \end{array} \right\} \quad (12)$$

Crack locations and depths can be determined by solving Eq.(12). In this work the PSO with increasing inertia weight is employed for this purpose, and its details are given in the next section.

### 2.3. The particle swarm optimization algorithm

PSO algorithm is initialized with a "swarm" composed of  $N$  particles. Particles refer to the candidate points in the search space of the optimization problem. To obtain the best solution each particle adjusts its trajectory toward its own previous best position and toward the previous best position of the swarm. By this way, each particle moves

in the search space with an adaptive velocity, and stores the best position of the search space. Location ( $x$ ) and velocity ( $v$ ) of a particle are updated with the following equations (Kennedy and Eberhart 1995; Parsopoulos and Vrahatis 2010)

$$\begin{aligned} v_{ij}^{k+1} &= v_{ij}^k + c_1 R_1 (p_{ij}^k - x_{ij}^k) + c_2 R_2 (p_{gj}^k - x_{ij}^k) \\ x_{ij}^{k+1} &= x_{ij}^k + v_{ij}^{k+1}, \quad i = 1, 2, \dots, N, \quad j = 1, 2, \dots, m, \quad k = 1, 2, \dots, K_{\max} \end{aligned} \quad (13)$$

where  $k$  is the iteration counter,  $K_{\max}$  denotes the maximum number of iterations,  $m$  is dimension of the problem,  $p_{ij}^k$  and  $p_{gj}^k$  are, respectively, the best positions of the  $i$ th particle and the swarm found until the  $k$ th iteration,  $R_1$  and  $R_2 \in U(0,1)$ , where  $U$  means the uniform random distribution,  $c_1$  and  $c_2$  are positive weighting constants called cognitive and social coefficients, respectively. These two constants regulate the relative velocity toward global and local best points. The algorithm using Eq.(13) is called standard PSO. On the other hand, Zheng et al. (2003) proposed an approach in which  $v_{ij}^k$  in Eq.(13) is multiplied with an inertia weight increasing from a lower value to an upper one iteratively. In their opinion, either global or local search ability associates with a small inertia weight, which possesses the capacity of exploring new space. Besides, a large inertia weight provides the algorithm more chances to be stabilized. According to this approach, velocity of each particle is updated as follows.

$$v_{ij}^{k+1} = w^k v_{ij}^k + \bar{c}_1 (p_{ij}^k - x_{ij}^k) + \bar{c}_2 (p_{gj}^k - x_{ij}^k) \quad \bar{c}_n = b_n R_n + d_n \quad (n=1,2) \quad (14)$$

where  $b_1 = b_2 = 1.5$ ,  $d_1 = d_2 = 0.5$ , and  $w^k$  is the inertia weight linearly increasing from 0.4 to 0.9, i.e.

$$w^k = 0.4 + (0.9 - 0.4) \frac{k}{K_{\max}} \quad (15)$$

In this study, this version of the PSO will be used since its stability and convergence speed are better than those of the classic PSO. The algorithm was executed in MATLAB environment. Initial values of particles and their velocities were obtained drawing random numbers within the range of each dimension (Trelea 2003), i.e.

$$x_{ij}^1 = x_{LB,j} + R.(x_{UB,j} - x_{LB,j}), \quad v_{ij}^1 = x_{LB,j} + R.(x_{UB,j} - x_{LB,j}) \quad (15)$$

where  $x_{LB,j}$  and  $x_{UB,j}$  are, respectively, the lower and upper boundary values of the  $j$ th dimension, and  $R \in U(0,1)$ . Besides, if a particle moves beyond ranges, then it is bounced back to the search space in the following way:

$$\left. \begin{aligned} x_{ij}^k &= x_{UB,j} - R.(x_{ij}^k - x_{UB,j}), & \text{if } x_{ij}^k > x_{UB,j} \\ x_{ij}^k &= x_{LB,j} + R.(x_{LB,j} - x_{ij}^k), & \text{if } x_{ij}^k < x_{LB,j} \end{aligned} \right\} \quad (16)$$

### 3. NUMERICAL SIMULATION

#### 3.1. Case studies

Using the same beam and vehicle parameters, the damage scenarios in Table 1 are considered. Road surface roughness is excluded for now, since its effect will be dealt with in the next section. To simulate the real situation, certain amount of noise is added to the reference data as follows (Zhu and Law 2006)

$$\bar{y}(z, t)_{\text{noisy}} = \bar{y}(z, t)_{\text{calc}} + N_p \cdot G \cdot \sigma \quad (17)$$

where  $\bar{y}(z, t)_{\text{calc}}$  is the calculated response of point  $z$  of the damaged beam (see Eq.(10)),  $N_p$  is the noise percentage,  $G$  is Gaussian distribution with zero mean and unit standard deviation,  $\sigma$  is the standard deviation of  $\bar{y}(z, t)_{\text{calc}}$ . Clearly, the first damage case in Table 1 is simpler than the second, since the dimension of the problem and the amount of noise are lower whereas crack size is bigger in the first case. Besides, the moving vehicle's speed is lower in the first case. This is significant, as the wavelet transform methods lose sensitivity to damage at higher moving load/vehicle speeds (Zhu and Law 2006; Nguyen and Tran 2010; Hester and Gonzalez 2011; Gökdağ 2011; Khorram et al. 2012). Thus, damage identification ability at higher speeds can be deemed as an advantage of the method.

Table 1. Damage scenarios.

Case	Crack Parameters	$V_p$ (m/s)	$N_p$ (%)
1	$\bar{z}_1 = 0.5, \bar{h}_1 = 0.3$	5	1
2	$\bar{z}_1 = 0.3, \bar{h}_1 = 0.1$ $\bar{z}_2 = 0.5, \bar{h}_2 = 0.1$ $\bar{z}_3 = 0.7, \bar{h}_3 = 0.1$	20	3

On the other hand, swarm size ( $N$ ) and the number of maximum iterations were determined by experience as  $N=20$  and  $K_{\text{max}} = 30$  for Case 1. These are selected as  $N=30$  and  $K_{\text{max}} = 60$  for Case 2, considering the dimension of the problem. Algorithm

was run ten times due to its stochasticity (Moradi et al 2011) for each case, and the results of the best runs are given in Table 2. Additionally, iterative variation of the objective function is given in Fig. 3 for the best runs. From Table 2 it is clear that the proposed method can successfully locate damage locations and estimate crack sizes for Case 1. Crack locations and depths are determined with the relative errors smaller than 1%. On the other hand, although the errors in the results are higher for Case 2, it is seen most of the parameters are determined with the error smaller than 10%. Especially, it is promising the errors in the damage locations are lower.

Table 2. Simulation results of the cases in Table 1.

Case		$\bar{z}_1$	$\bar{z}_2$	$\bar{z}_3$	$\bar{h}_1$	$\bar{h}_2$	$\bar{h}_3$	$f^*$
1	Exact	0.5000	---	---	0.3000	---	---	0.1174
	Predicted	0.4994	---	---	0.3004	---	---	0.1241
	$\varepsilon$	0.12	---	---	0.12	---	---	5.7
2	Exact	0.3000	0.5000	0.7000	0.1000	0.1000	0.1000	0.0906
	Predicted	0.3293	0.4948	0.6723	0.1090	0.0750	0.1099	0.0911
	$\varepsilon$	9.75	1.04	3.95	9.01	25.00	9.85	0.55

\*: See Eq. (10),  $\varepsilon := 100 \times |E - Pr| / E$ , E: Exact, Pr: Predicted

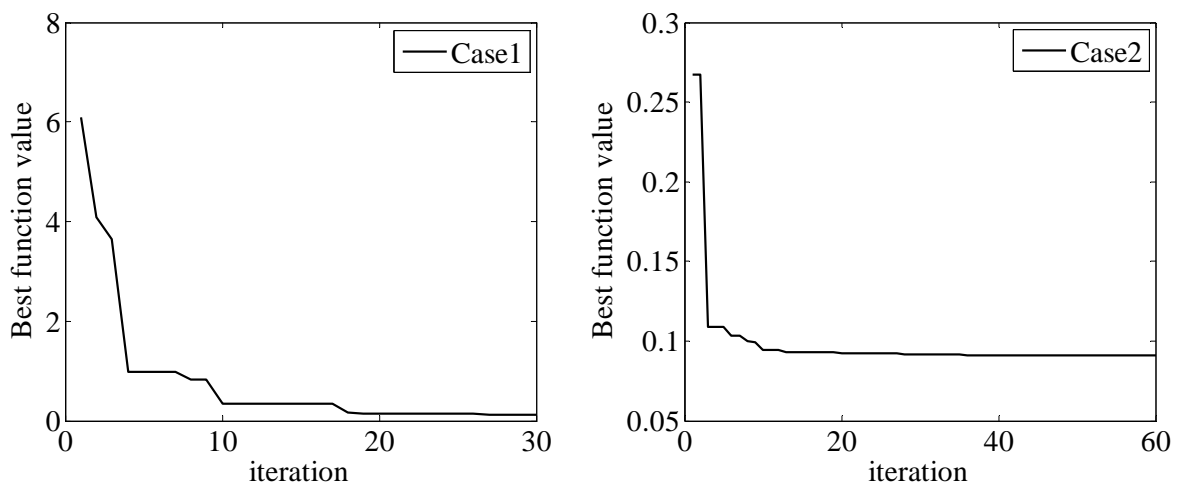


Fig. 3. Variation of objective function with iteration.

### 3.2. Effect of road surface roughness

As indicated previously road surface roughness has great impact on the dynamic response of the system (see Fig.2). Since roughness function is random, each

measurement produces different deflection profile (Wu and Law 2011), i.e.  $\bar{y}$  in Eq.(10). Let's indicate this considering Case 2 in Table 1. Fig. 4 illustrates ten deflection time histories of the midspan with  $S_d(f_0) = 6 \times 10^{-6}$ . It is seen that each curve is different from the others due to the stochasticity of the roughness function. Thus, the proposed method cannot be implemented with single deflection profile recorded from measurement point. Fortunately, the roughness function in Eq.(4) has Gaussian distribution, i.e. a stochastic process composed of many roughness functions has the probability density function which is well correlated with that of the Gaussian process (Wu and Law 2011). Thus, if deflection time history of a point on the damaged beam is measured many times and averaged, then the mean value of the deflections becomes closer to the one obtained by ignoring the roughness and noise, i.e. the function  $y$  in Eq.(10). This is illustrated in Fig. 5 for the same case. The right-side figure indicates that the more the number of averages, the better the correlation between the computed and average deflections, i.e.  $y$  and  $\bar{y}$ . In the left-side figure the average value of 30 measured deflection profiles (curve II) and the reference one computed by the mathematical model (curve I) are compared. It is obvious that not only the average curve is well correlated with the reference one but also noise is eliminated to a great extent by averaging. Now, employing the average of 50 deflection profiles from each measurement point, the optimization problem is solved again, and the results in Table 3 are obtained. At the table the mean value of the ten values are given for each variable and the objective function, since each run of the optimization algorithm yielded erroneous results. From the table, it is seen that crack locations and depths are determined with error smaller than 10%. Thus, we can say that employing the average values of measured deflections enhances the accuracy of the proposed method.

Table 3. Simulation results of Case 2 in Table 1 including road surface roughness.

	$\bar{z}_1$	$\bar{z}_2$	$\bar{z}_3$	$\bar{h}_1$	$\bar{h}_2$	$\bar{h}_3$	$f^*$
Exact	0.3000	0.5000	0.7000	0.1000	0.1000	0.1000	0.0273
Predicted	0.2748	0.5395	0.7652	0.1099	0.1097	0.0907	0.0254
$\varepsilon$	8.4	7.9	9.3	9.8	9.7	9.3	6.9

\*: Eq. (10),  $\varepsilon = 100 \times |E - Pr| / E$ , E: Exact, Pr: Predicted.

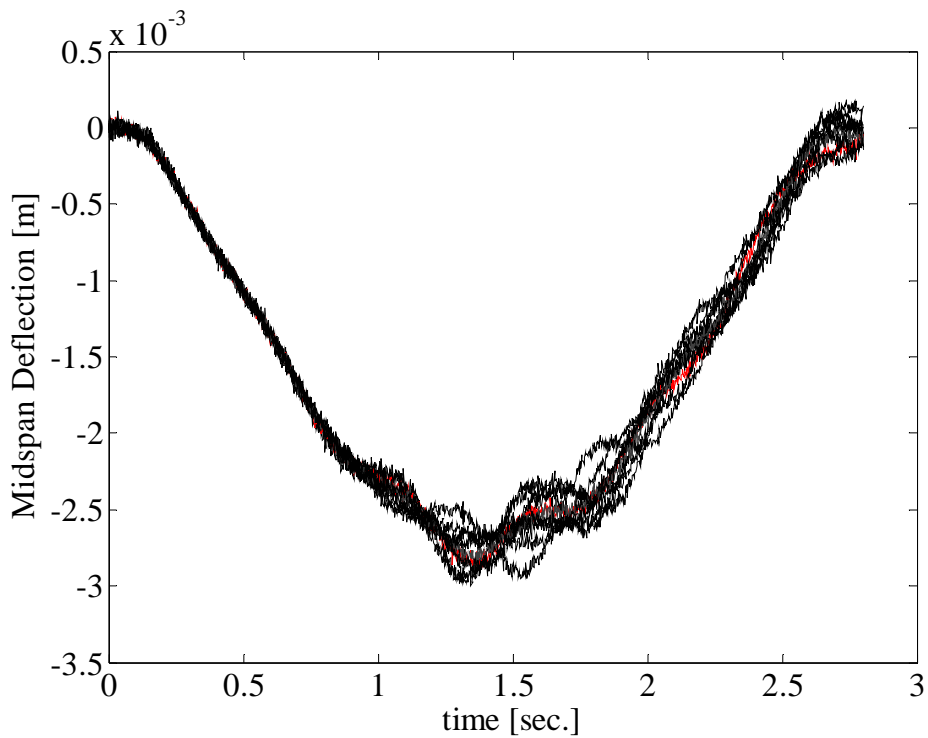


Fig. 4. Midspan deflections of the beam corresponding to ten different roughness profiles.

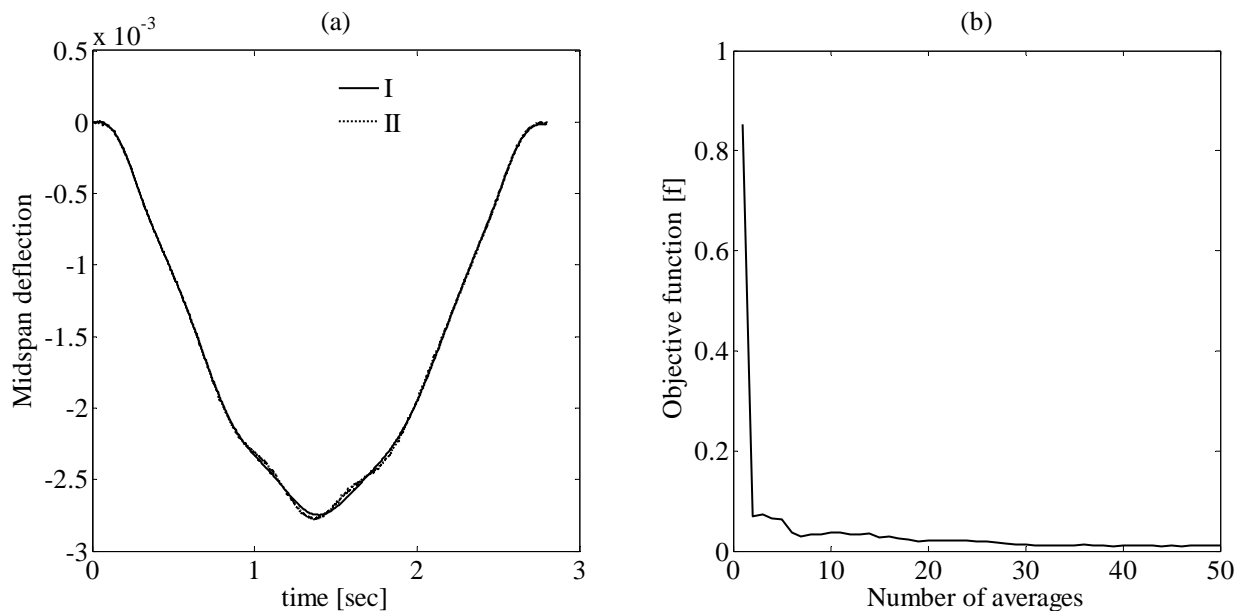


Fig. 5. (a): Comparison of midspan deflections for Case 2 in Table 1 (I: no noise and roughness, II: Average of 30 deflection curves including noise and roughness). (b): Variation of objective function with the number of averages (only the midspan deflection is employed, i.e.  $N_{mp} = 1$  in Eq.(10)).

## CONCLUSION

In this study, a new crack identification method for beam type structures carrying moving vehicle is proposed. Damage detection was formulated as an inverse problem using the difference of measured time dependent deflections of the damaged beam and those computed by the mathematical model of the structure. Then, this problem was solved through a robust evolutionary algorithm, i.e. the particle swarm optimization with increasing inertia weight, for crack locations and depth. Both road surface roughness and measurement noise are considered. It was demonstrated that crack size of 0.1 can be determined by the proposed approach with error lower than 10%. The drawback of the method is that it is difficult, by a single measurement, to obtain the reference data well-correlated with the one computed by the mathematical model of the structure. This is because of the random nature of the road surface roughness, which gives rise to different deflection profiles at every measurement. However, average of multiple measurements is well-correlated with the one computed by the mathematical model. Thus, the proposed method can be implemented provided the average of multiple measurements is employed as reference. Future works are planned to consider the opening and closing of crack during the simulation, and test the method with real data.

## REFERENCES

- Ariaei, A., Ziaei-Rad, S., and Ghayour, M. (2009), "Vibration analysis of beams with open and breathing cracks subjected to moving masses", *Journal of Sound and Vibration*, Vol. **326**, 709-724.
- Begambre, O. and Laier, J.E. (2009), "A hybrid particle swarm optimization – simplex algorithm (PSOS) for structural damage identification", *Advances in Engineering Software*, Vol. **40**, 883-891.
- Bilello, C. and Bergman, L.A. (2004), "Vibration of damaged beam under a moving mass: theory and experimental validation", *Journal of Sound and Vibration*, Vol. **274**, 567-582.
- Buezas, F.S., Rosales, M.B. and Filipich, C.P. (2010), "Damage detection with genetic algorithms taking into account a crack contact model", *Engineering Fracture Mechanics*, doi:10.1016/j.engfracmech.2010.11.008.
- Clough, R.W. and Penzien, J. (1995), *Dynamics of Structures*, Computers & Structures, Inc., Berkeley, CA.
- Fřyba, L. (1999), *Vibration of Solids and Structures Under Moving Loads*, Telford, London.
- Gökdağ, H. (2011), "Wavelet-based damage detection method for a beam-type structure carrying moving mass", *Structural Engineering and Mechanics*, Vol. **38**(1), 81-97.

- Hester, D. and Gonzalez, A. (2011), "A wavelet-based damage detection algorithm based on bridge acceleration response to a vehicle", *Mechanical Systems and Signal Processing*, doi:10.1016/j.ymssp.2011.06.007.
- Kennedy, J. and Eberhart, R. (1995), "Particle swarm optimization", *Proceedings of the 4th IEEE International Conference on Neural Networks*, Vol. **4**, 1942-1948.
- Khorram, A., Bakhtiari-Nejad, F. and Rezaeian, M. (2012), "Comparison studies between two wavelet based crack detection methods of a beam subjected to a moving load", *International Journal of Engineering Science*, Vol. **51**, 204-215.
- Law, S.S. and Zhu, X.Q. (2004), "Dynamic behavior of damaged concrete bridge structures under moving vehicular loads", *Engineering Structures*, Vol. **26**, 1279-1293.
- Mahmoud, M.A. (2001), "Effect of cracks on the dynamic response of a simple beam subject to a moving load", *Proceedings of the Institution of Mechanical Engineers*, Vol. **215**, 207-215.
- Moradi, S., Razi, P. and Fatahi, L. (2011), "On the application of bees algorithm to the problem of crack detection", *Computers and Structures*, Vol. **89**, 2169-2175.
- Nguyen, K.V. and Tran, H.T. (2010), "Multi-cracks detection of a beam-like structure based on the on-vehicle vibration signal and wavelet analysis", *Journal of Sound and Vibration*, Vol. **329**, 4455-4465.
- Parsopoulos, K.E. and Vrahatis, M.N. (2010), *Particle swarm optimization and intelligence: Advances and Applications*, IGI Global, Hershey PA.
- Seyedpoor, S.M. (2012), "A two stage method for structural damage detection using a modal strain energy based index and particle swarm optimization", *International Journal of Non-Linear Mechanics*, Vol. **47**, 1-8.
- Trelea, I.C. (2003), "The particle swarm optimization algorithm: convergence analysis and parameter selection", *Information Processing Letters*, Vol. **85**, 317-325.
- Wu, S.Q. and Law, S.S. (2011), "Vehicle axle load identification on bridge deck with irregular road surface profile", *Engineering Structures*, Vol. **33**, 591-601.
- Zhu, X.Q., and Law, S.S. (2006), "Wavelet-based crack identification of bridge beam from operational deflection time history", *International Journal of Solids and Structures*, Vol. **43**, 2299-2317.
- Zheng, Y-L., Ma, L-H., Zhang, L-Y. and Qian, J-X. (2003), "On the convergence analysis and parameter selection in particle swarm optimization", *Proceedings of the 2nd International Conference on Machine Learning and Cybernetics*, Vol. **3**, 1802-1807.